

Detection of Ammonia Gas Molecules in Aqueous Medium by Using Nanostructured Ag-Doped ZnO Thin Layer Deposited on Modified Clad Optical Fiber

Shailendra K. Singh,* Debjit Dutta, Anirban Dhar, Shyamal Das, Mukul C. Paul, and Tarun K. Gangopadhyay

The synthesis of Ag-doped ZnO nanorod employing hydrothermal process over modified cladd optical fiber is reported. The developed material is characterized using X-ray diffraction (XRD), Fourier transformed infrared spectroscopy (FTIR), X-ray photoelectron spectroscopy (XPS), field emission scanning electron microscopy (FESEM), and Brunauer-Emmett-Teller (BET) analysis to evaluate the morphology and the nature of nanorod formed. The initial performance of the coated modified clad optical fiber toward detection of ammonia gas in aqueous solution is also presented. The sensing performance revealed that the developed material possess improved sensitivity toward ammonia gas at room temperature compared to Ag doped nanowires containing optical fiber sensor.

electrons ($200 \text{ cm}^2 \text{ V s}^{-1}$), large surface area suitable for gas adsorption and anisotropic properties.^[5,6] Due to these unique characteristics of ZnO, it was deposited on the optical fiber for the detection of ethanol,^[7] ammonia,^[8] humidity,^[9] etc.

Pure ZnO shows weak optical properties that causes point defects such as oxygen vacancies or interstitial Zn, so it cannot use directly into the industry. In order to make optoelectronic devices based on ZnO, formation of p type and n type states are essential.^[10] However, doping of noble metals like Ag,^[4,11] Au, Pt, Pd etc. are co-doped with ZnO in order to enhance the surface area and electronic properties to achieve improved sensing performances.

1. Introduction

Research activity related to nanostructured metal oxides are gaining a lot of attraction in recent years as in general nanostructured material possesses high surface area to volume ratio and exhibit novel optical, chemical as well as electronic properties. In this respect, ZnO is a well known n-type semiconductor material having wide band gap (3.37 eV), large binding energy (60 mV), excellent chemical and thermal stability^[1] and good biocompatibility. The ZnO can exist in different forms such as nanowires,^[2] nanorods,^[3] nanoellipsoids^[4] and many other nanostructures synthesized through different process viz. homogeneous precipitation, sonochemical method, direct synthesis, hydrothermal process, direct precipitation, reverse micelles etc. Among different possible applications viz. photo catalysis, dye-sensitized solar cells, gas sensors, solid state optoelectronic devices etc. gas sensing is one of the important area thanks to its high mobility of conduction

Silver is being widely used as a dopant which activates the chemical analytes to accelerate the chemical reaction, catalytic activity and catalytic oxidation and is one of the best promising candidates to dope with ZnO because of its high solubility, large ionic size and minimum orbital energy. Doping of Ag in ZnO, forms an impurity band between orbitals of Ag and O-2p orbital, which shifted the Fermi level towards valence band and induced p type properties in ZnO. The p type properties depend on Ag content, electrochemical growth and post annealing conditions.^[10,12] Ag co-doping with [Ag/graphene],^[13] [Ag nanoparticles/poly(vinyl alcohol)]^[14] are reported in order to achieve enhanced sensitivity, fast response, good stability, and expected to exhibit enhanced optical, electrical, and magnetic properties. The nanorods with Ag doping have more surface to volume ratio than Ag doped nanoparticles. So nanorods and nanowires have more sensing capacity than nanoparticle.^[5,15]

Ammonia sensors have developed using metal oxides,^[16] carbon nanotubes,^[17] and polymers.^[18] Very recently, Marcel Bouvet et al. have reported a new kind of ammonia sensor (10–100 ppm) by using organic n-type molecular semiconductor materials namely triphenyldioxazine and lutetium bisphthalocynnine.^[19] Metal oxide based sensors have problem with room temperature, high power consumption, and reusability. However, the optical fiber sensor has advantages over metal based thin film. The optical fiber sensor is more attractive due to fast response and room temperature operation^[20] and remote sensing ability.^[21] There are various techniques to design a sensor, but one of the popular techniques is to design a modified cladding with a suitable optical fiber coating on the fiber.^[22–24]

S. K. Singh, Dr. A. Dhar, Dr. S. Das, Dr. M. C. Paul, Dr. T. K. Gangopadhyay
Academy of Scientific and Innovative Research (AcSIR)
Ghaziabad-201002, India
E-mail: shailendra03eie@gmail.com

S. K. Singh, Debjit Dutta, Dr. A. Dhar, Dr. S. Das, Dr. M. C. Paul,
Dr. T. K. Gangopadhyay
Fiber Optics and Photonics Division
CSIR-Central Glass & Ceramic Research Institute
196, Raja S. C. Mullick Road, Jadavpur, Kolkata-700032, India

DOI: 10.1002/pssa.201900141

Based on the above background, here we present the preparation of Ag/ZnO nanorod coated fiber probe and evaluated their sensing performance towards ammonia gas. The coating materials have been synthesized by conventional hydrothermal process and as-synthesized materials were characterized by X Ray Diffraction (XRD), Fourier Transform Infra Red Spectroscopy (FTIR), X ray Photoelectron Spectroscopy (XPS) and the morphology of the coated fiber was checked employing by Field Emission Scanning Electron Microscopy (FESEM). Finally the initial performance of developed sensor probe towards ammonia sensing was also evaluated.

2. Experimental Details

2.1. Synthesis of ZnO and Ag/ZnO Nanorod

The synthesis of ZnO and Ag/ZnO nanorod over fiber surface was carried out in a two stage process as mentioned below.

Different chemical used during preparation consists of Zinc acetate dihydrate $(\text{CH}_3\text{COO})_2\text{Zn} \cdot 2\text{H}_2\text{O}$ (Merck, Germany $\geq 98\%$), Zinc nitrate hexahydrate $\text{Zn}(\text{NO}_3)_2 \cdot 6\text{H}_2\text{O}$ (Merck, Germany $\geq 96\%$), Hexamethylenetetramine $(\text{CH}_2)_6\text{N}_4$ (Merck, Germany $\geq 99.5\%$), Silver Nitrate AgNO_3 (99.995%) (Merck, Germany), Ammonia (NH_3) (Merck, Germany 25%), and ethanol $(\text{C}_2\text{H}_5\text{OH})$ (Merck, Germany). We have used a multimode fiber fabricated in house having NA 0.15 having core diameter of $45 \mu\text{m}$. Prior to deposition of chemicals over fiber cladding, a small portion ($\approx 1 \text{ cm}$) of the cladding layer was etched using 48% HF solution with optimized process parameters and then placed on hot plate maintaining a temperature of 70°C . In the first stage, a seed layer of ZnO is made over the fiber surface which is essential to achieve uniform growth of nanorod in subsequent stages. An ethanolic solution containing Zinc acetate was then dropped over the etched fiber surface followed by drying at 350°C for about 2 h.

In the second stage, hydrothermal technique was employed to achieve the nanorod growth formation over the ZnO coated modified clad optical fiber. In an autoclave, an equal concentration comprised of $(0.05 \text{ M}) \text{Zn}(\text{NO}_3)_2 \cdot 6\text{H}_2\text{O}$ and Hexamethylenetetramine dissolved in 60 mL of deionised (DI) water under stirring, where ZnO seed layer coated fiber is dipped and heated at 90°C for 1 h. The coated fiber was finally rinsed with DI water and dried for one day prior to evaluate its sensing performance.

Similar experiments were performed to prepare Ag/ZnO nanorod coated fiber probe where all experimental conditions remain same except we additionally used AgNO_3 instead of $\text{Zn}(\text{NO}_3)_2 \cdot 6\text{H}_2\text{O}$ along with other reactants mentioned above.

The optimization of the coating thickness of Ag/ZnO coating over the clad modified fiber is important. However, we could not measure the exact thickness of the coated layers but in order to optimize the sensing performance a number of sensor probes were fabricated where number of dipping was varied from 1 to 4 times which means our coating thickness remain within micron range.

3. Characterization of Pure ZnO and Ag/ZnO

The crystalline structure of synthesized material was examined by XRD using a D8 advanced Davinci (Bruker) XRD system

where Cu K α radiation (0.15418 nm) used in the 2θ range from 20° to 90° . The emission spectra of ZnO and Ag/ZnO was examined by FTIR. The impurities of the coated material were checked by the XPS. The morphology of hexagonal nanorod on fiber was checked by FESEM [Supra35 VP(Carl Zeiss)].

3.1. Structural Analysis

XRD analysis was performed checking the crystallinity of Zn and Ag in the synthesized materials. The XRD patterns of synthesized pure ZnO nanorod and Ag/ZnO nanorod are shown in **Figure 1a** to **b**. All the peaks were indexed with ZnO and matched well with JCPDS file (no. 36-1451). The peaks at 31.79° , 34.56° , 36.27° , 38.23° , 44.41° , 56.65° , 62.66° , 64.52° , 66.33° , 67.33° , 68.13° , and 72.56° , which corresponds to the (h,k,l) planes of (100), (002), (101), (111), (102), (103), (220), (200), (112), (201), and (004) patterns correspond to the hexagonal nanorod growth of ZnO. The peaks observed at 38.23° , 44.21° , and 64.52° confirms Ag in the ZnO and matched well with JCPDS file (no. 04-0783).^[25–27]

3.2. FTIR Analysis

FTIR analysis was performed to evaluate the mode of bond in Ag and ZnO present in synthesized materials. The FTIR spectra of pure ZnO and Ag/ZnO nanorod were analysed at room temperature. KBr pellet method was used to measure the sample by using Nicolet 380 FTIR spectrometer. The broad absorption band at 3377 cm^{-1} is due to O-H bending vibration of water and at 1381 cm^{-1} is due to NO_3^- groups.^[25] The peaks at 496 cm^{-1} is assigned for Ag/ZnO and at 548 cm^{-1} is due to oxygen vacancies.^[5,27]

If we compare both graphs **Figure 2a** and **b**, we observed that Ag/ZnO materials which makes the peaks of pure ZnO at wavenumber 831 cm^{-1} . This indicates that developed material is not purely crystalline.

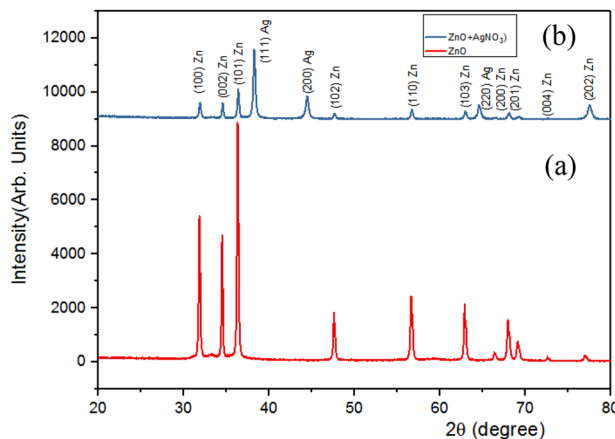


Figure 1. XRD pattern of (a) as-prepared ZnO (b) Ag-doped ZnO.

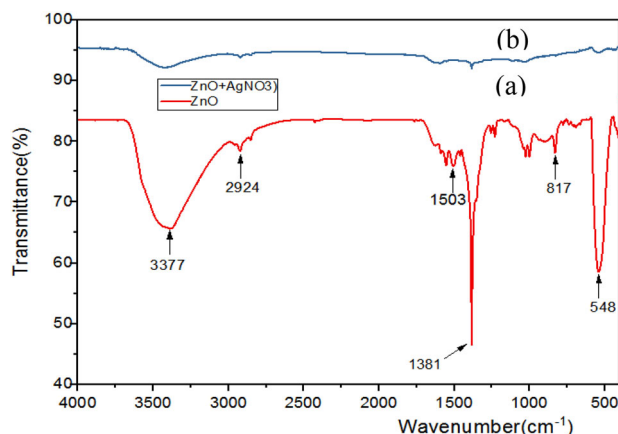


Figure 2. FTIR spectra of (a) as-prepared ZnO (b) Ag/ZnO.

3.3. XPS Analysis

XPS analysis was done to analyze the oxidation state of the chemical elements in pure ZnO and Ag/ZnO nanorods. **Figure 3a** shows the full scan spectrum of as growth of ZnO and Ag/ZnO nanorods. The peaks observed in the spectra are Zn, C, O, and Ag, i.e., no impurities were found. Baseline correction was performed to fit the relevant peaks of ZnO and Ag/ZnO. In **Figure 3b**, the O 1s peak at the lowest binding energy was assigned to 529.76 eV which indicates that O is in metal oxide (ZnO) forms. The binding energy at 531.52 eV, and 529.76 eV indicates that O is in O⁻ and O⁻² forms. The peak binding energy at 1021.43 eV and 1044.51 eV corresponds to peak of Zn 2p_{3/2} and Zn 2p_{1/2} respectively.^[12] It indicates the existence of divalent oxidation state in pure ZnO. The two peaks of binding energy 367.51 eV and 373.51 eV which corresponds to Ag 3d_{5/2} and Ag 3d_{3/2} of Ag/ZnO nanorods morphology. The experimental peak of Ag 3d overlaps with fitted value. It indicates that the density of Ag is constant.^[4] XPS indeed exhibit chemical shifts towards the higher binding energy (BE) by 23.1 eV with corresponding peaks 2p_{3/2} and 2p_{1/2}. The shift in peaks is due to Ag ionic radii enhancement. The peaks 2p_{3/2} and 2p_{1/2} shifted with BE ≈ 0.36 eV after Ag doping in ZnO. In **Figure 3f** the bulk atomic ratio of Ag/ZnO was found 26.45/73.55 by XPS. In XPS fitting besides 2p_{1/2} all other peaks of Zn was discarded which in turn enhances Ag: ZnO ratio.

3.4. Microstructural Analysis

FESEM microstructural analysis was carried out to evaluate the morphology of deposited materials and uniformity of coating achieved. The nanorods grown on fiber is suitable for gas sensing due to its large surface area. FESEM reveals that nanorods are vertically arranged on the cylindrical surface of the optical fiber. When it interacts with gas species, gas can penetrate to the bottom portion of coated fiber to give maximum response. The morphology of ZnO and Ag/ZnO nanocomposite were analysed by FESEM. Through this analysis, we observed that hexagonal nanorod formed on the surface of optical fiber. The average size of hexagonal nanorods was found to be ≈ 200 nm for

ZnO but for Ag/ZnO it reduces to (≈ 100 nm). In **Figure 4a** and **d** represents nanostructure formation of ZnO and Ag/ZnO on the fiber. In **Figure 4b** and **e**, hexagonal nanorod growth was shown on the surface of optical fiber and **Figure 4c** and **f** represents the Energy Dispersive of X-Ray Spectroscopy (EDX) plot of ZnO and Ag/ZnO. These elemental peaks prove that there is no impurity in these coated fibers. Comparison of **Figure 4b** and **e** clearly indicates that for the same area under investigation the total number of open channels are approximately 3X times in Ag/ZnO than synthesized pure ZnO. The bulk atomic ratio of Ag/ZnO is found to be 21.9:78.1 from EDX.

3.5. Brunauer-Emmett-Teller (BET) Analysis

To investigate the surface area of the materials studied N₂ sorption analysis was performed. The BET specific surface area of Ag/ZnO materials namely 3%, 6%, 9% doping Ag was found to be 2.535 m² g⁻¹, 4.359 m² g⁻¹, and 2.027 m² g⁻¹ respectively from the nitrogen absorption isotherm. For 6% Ag/ZnO sample total pore volume is 6.186 $\times 10^{-2}$ cc g⁻¹ and pore size is smaller than 328.5 nm diameter at P/P₀ = 0.99414. This comparative analysis was performed to select the best sensing materials (here 6% Ag/ZnO sample) among the three samples fabricated discussed here. We observed enhancement of surface area for 6% sample than 3% but it decreases again for 9% sample which could be due to clustering of Ag over ZnO surface.^[28]

4. Result and Discussions

4.1. Experimental Set Up

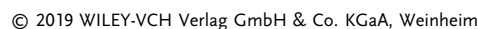
The schematic diagram for ammonia detection set up in water medium is shown in the **Figure 5**. Tungsten halogen white light source (330–1800 nm) was launched through one end of Ag/ZnO nanorod coated fiber. The light propagates through the optical fiber was collected by the IR (InGaAs) detector within wavelength range of 1000–1800 nm. We have measured ammonia concentrations in aqueous solution from 0 to 450 parts per million (ppm) in a repeated manner.

The Equation (1) was used to calculate the value of ammonia in ppm (Merck, Germany) by adding drops of NH₃ quantitatively.

$$\text{ppm} = \frac{\text{mass of solute}}{\text{mass of solution}} \times 10^6 \quad (1)$$

4.2. Sensing Principle

Figure 5b presents schematic of modified clad optical fiber where the light propagates into the core of fiber through principle of total internal reflection (TIR). The light propagates in optical fiber which propagates into the cladding during TIR known as evanescent field and it interacts between air and cladding. The evanescent field exponentially decaying in the nature from core to cladding. But when the cladding is coated



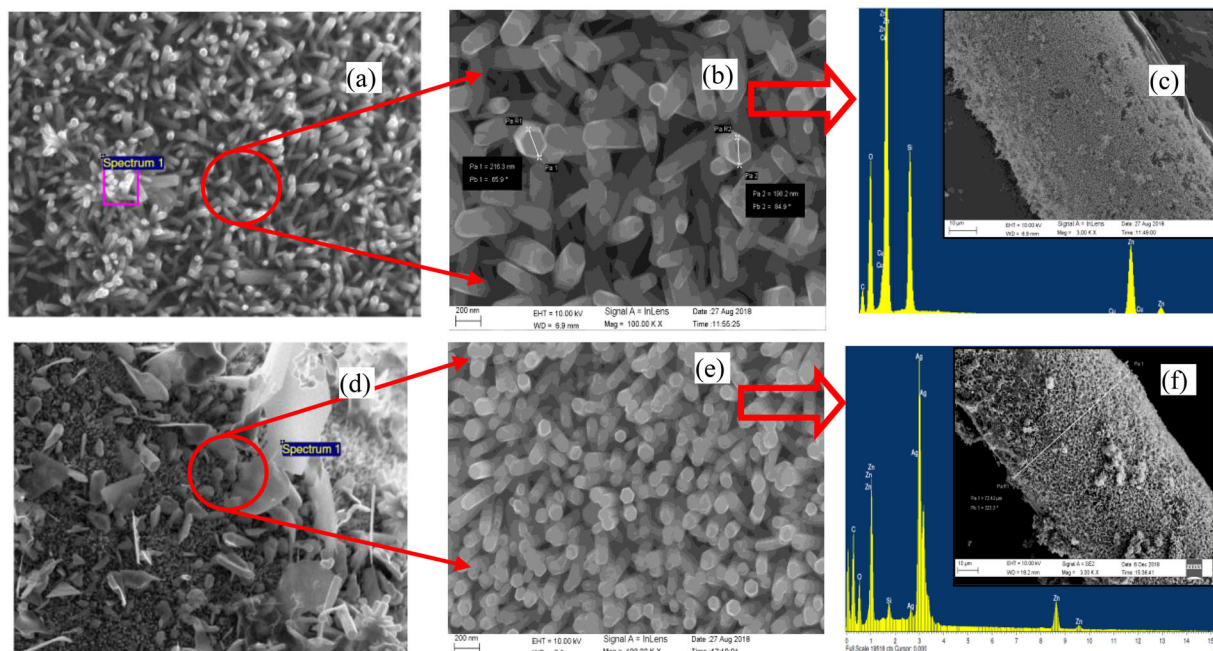
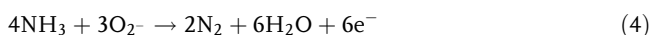


Figure 4. FESEM image of (a) Pure ZnO coated optical fiber, b) Hexagonal nanorod growth on ZnO coated optical fiber, c) The EDX pattern of ZnO coated optical fiber, d) Ag/ZnO coated fiber, (e) Hexagonal nanorod growth on Ag/ZnO coated fiber, f) The EDX pattern of Ag/ZnO coated fiber.



4.3. Spectral Analysis

During the experiments, the output intensity of sensor in ambient air is taken as a reference. The sensor is dipped in

100 mL of DI water and measured quantity of ammonia is added through micropipette. We recorded the data after 10 min interval and noticed that the power intensity is decreased. The spectral power intensity change for different concentration was shown in **Figure 6a** which shows zoom view of the circled portion of Figure 6a from the wavelength of 1240–1280 nm. The sensitivity of the clad modified optical sensor is related to changes in output intensity. It is defined by following equations.

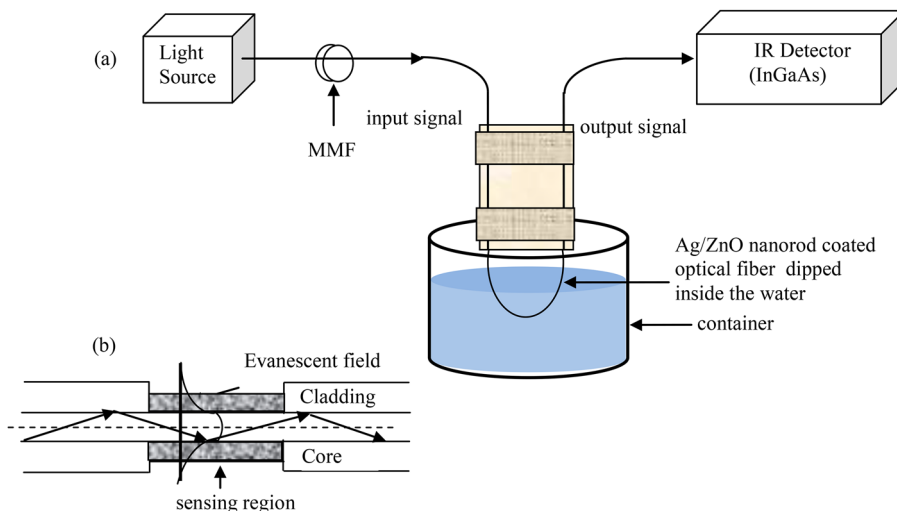


Figure 5. The schematic diagram of (a) the experimental set up for detection of NH_3 in water medium. b) Modified cladding portion of the sensing probe.

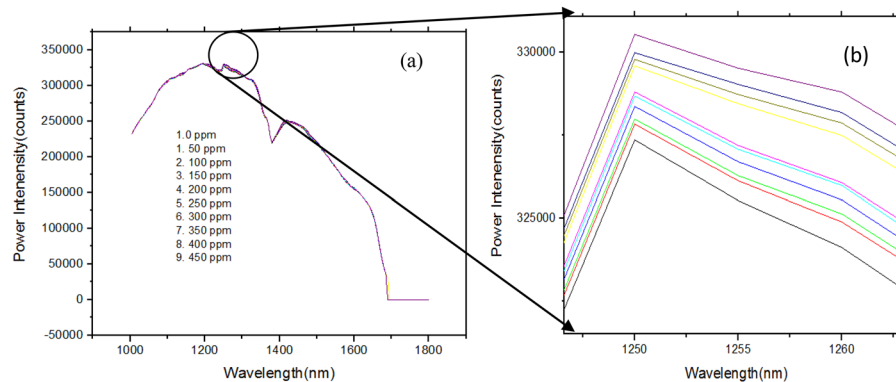


Figure 6. Spectral response of clad modified optical fiber gas sensor based on Ag-doped ZnO nano-rods for different concentrations of ammonia gas (a). The variations of Power Intensity with wavelength (b). Enhanced view of the sensing region.

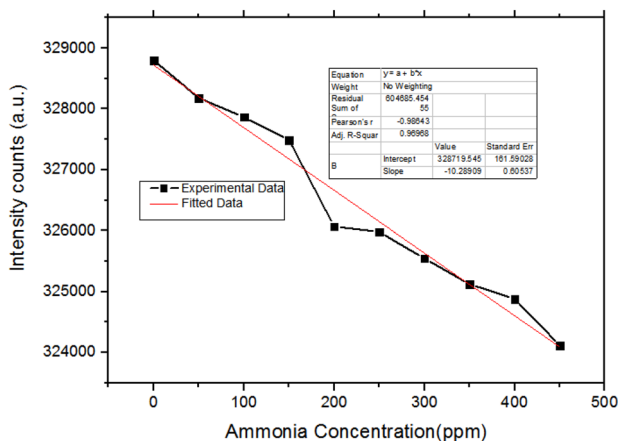


Figure 7. Power Intensity (dB) variation with NH_3 concentration from (0–450) ppm.

$$\text{Sensitivity} = \left(\frac{I_0 - I_p}{I_0} \right) \times 100 \quad (5)$$

where, I_0 is the signal intensity in the absence of analyte and I_p is the signal intensity in the presence of analytes. The sensitivity (%) of the sensor was found to be 0.435 and found to be better over the previously reported value indicating its potential NH_3

sensing in aqueous solution. The sensitivity of present system is, however, less than that of tapered fiber^[14] where evanescent field travel more inside the cladding whose magnitude exponentially decreases from core to cladding. Nevertheless, in terms of mechanical stability the present fiber system is more acceptable in terms of practical application point of view.

The power intensity decreases with increase of ammonia gas concentration was shown in the **Figure 7** and it is linearly varies with ammonia concentration. This again indicates that the developed Ag/ZnO nanorod coated fiber is a potential candidate for ammonia sensing in aqueous solution.

Comparison of gas sensing performance of various materials on modified clad fiber towards ammonia sensor is shown in **Table 1**.

5. Conclusion

In summary, we report here a successful synthesis of Ag-doped ZnO nanorod by hydrothermal technique in a two step process over modified clad optical fiber. The characterization of developed materials was performed by XRD, FTIR, XPS, and FESEM. The as synthesized materials was coated on fiber by autoclave techniques. FESEM reveals that nanorods size on Ag/ZnO nanorod coated fiber is smaller than pure ZnO coated fiber. Thus Ag/ZnO coated fiber is more suitable due to the presence

Table 1. Comparison of ammonia gas sensing performance reported.

	Sensor type	Sensitivity ammonia (counts/ppm)
	Clad modified	0.435 (present work)
Ag doped ZnO nanorods		
Silver nanowires ^[2]	Clad modified	0.17
Silver nanoparticles (Ag 1.3%) ^[11]	Tapered fiber	0.32
Silver nanoparticles (Ag 3.3%) ^[11]	Tapered fiber	0.59
Silver nanoparticles (Ag 6.6%) ^[11]	Tapered fiber	0.88
Amin func.ZnO nanoflakes ^[28]	Clad modified	0.262
Silver nanoparticles ^[31]	Clad modified	0.12
ZnO nanocrystalline ^[32]	Clad modified	0.24

of more open channels as reveal from FESEM analysis for gas sensing applications. The change in power signal around 1240–1280 nm with change in NH_3 concentration indicates its potential towards NH_3 sensing in aqueous solution. The maximum sensitivity (%) of the proposed sensor is found to be 0.435 at room temperature.

Acknowledgements

Shailendra Kumar Singh is a CSIR NET SRF and is very thankful to CSIR HRDG for providing fellowship and gratefully acknowledge to Advanced material characterization division of CSIR-CGCRI, Kolkata for the help of material characterizations.

Conflict of Interest

The authors declare no conflict of interest.

Keywords

ammonia sensing, material characterization, optical fiber, synthesis of Ag/ZnO nanocomposite, synthesis of ZnO nanorod

Received: February 25, 2019

Revised: April 30, 2019

Published online:

- [1] L. Vayssieres, *Adv. Mater.* **2003**, 15, 464.
- [2] L. R. Shobin, D. Satikumar, S. Manivannan, *Sens. Actuators A* **2014**, 214, 74.
- [3] J. Xu, Y. Zhang, Y. Chen, Q. Xiang, Q. Pan, L. Shi, *Mater. Sci. Eng. B* **2008**, 1500, 55.
- [4] R. Sankar Ganesh, M. Navaneethan, V. L. Patil, S. Ponnusamy, C. Muthamizhchelvan, S. Kawasaki, P. S. Patil, Y. Hayakawa, *Sens. Actuators B* **2018**, 255, 672.
- [5] Q. Xiang, G. Meng, Y. Zhang, J. Xu, P. Xu, Q. Pan, W. Yu, *Sens. Actuators B* **2010**, 143, 635.
- [6] B. Gong, T. Shi, W. Zhu, G. Liao, X. Li, J. Huang, T. Zhou, Z. Tang, *Sens. Actuators B* **2017**, 245, 821.
- [7] M. Konstantaki, A. Klini, D. Anglos, S. Pissadakis, *Opt. Express* **2012**, 20, 84729.
- [8] B. Renganathan, D. Sastikumar, G. Gobi, N. Rajeswari Yogamalar, A. Chandra Bose, *Opt. Laser Technol.* **2011**, 43, 1398.
- [9] F. Fang, J. Futter, A. Markwitz, J. Kennedy, *Nanotechnology* **2009**, 20, 245502.
- [10] S. M. Hosseini, I. Abdolhosseini Sarsari, P. Kameli, H. Salamati, *J. Alloy Compd.* **2015**, 640, 408.
- [11] S. Devendiran, D. Sastikumar, *Opt. Laser Technol.* **2017**, 89, 186.
- [12] O. Lupan, L. Chow, L. K. Ono, B. Roldan Cuenya, G. Chai, H. Khallaf, S. Park, A. Schulte, *J. Phys. Chem.* **2010**, 114, 12401.
- [13] A. Aziz, H. N. Lim, S. H. Girei, M. H. Yaacob, M. A. Mahdi, N. M. Huang, A. Pandikumar, *Sens. Actuators B* **2015**, 206, 119.
- [14] D. Ritesh Raj, S. Prasanth, T. V. Vineeshkumar, C. Sundarsanakkumar, *Opt. Commun.* **2015**, 340, 86.
- [15] C.-Y. Lin, Y.-H. Lai, A. Balamurugan, R. Vittal, C.-W. Lin, K.-C. Ho, *Talanta* **2010**, 82, 340.
- [16] K. K. Makhija, A. Ray, R. M. Patel, U. B. Trivedi, H. N. Kapse, Indian Academy of Sciences, *Bull. Mater. Sci.* **2005**, 28, 9.
- [17] M. Eising, C. E. Cava, R. V. Salvatierra, A. José, G. Zarbin, L. S. Roman, *Sens. Actuators B* **2017**, 245, 25.
- [18] Z. Jin, Y. Su, Y. Duan, *Sens. Actuators B* **2017**, 245, 25.
- [19] A. Wannebroucq, G. Gruntz, J.-M. Suisse, Y. Nicolasb, R. Meunier-Prest, M. Mateos, T. Toupance, M. Bouvet, *Sens. Actuators B Chem.* **2018**, 255, 1694.
- [20] A. Paliwal, A. Sharma, M. Tomar, V. Gupta, *Sens. Actuators B* **2017**, 250, 679.
- [21] S. Bagchi, R. Achla, S. K. Mondal, *Sens. Actuator B* **2017**, 250, 52.
- [22] R. K. Mondal, D. Dutta, S. Das, A. Dhar, M. C. Paul, *J. Chemists* **2016**, 88, 1.
- [23] K. Yamini, B. Renganathan, A. R. Gnaesan, T. Prakash, *Opt. Fiber Technol.* **2017**, 36, 139.
- [24] T. Subashini, B. Renganathan, A. Stephen, T. Prakash, *Mater. Sci. Semiconductor Process.* **2018**, 88, 181.
- [25] A. A. Ibrahim, G. N. Dar, S. A. Zaidi, A. Umar, M. Abaker, H. Bouzid, S. Baskoutas, *Talanta* **2012**, 93, 257.
- [26] C. Hong, Q. Zhou, Z. Lu, A. Umar, R. Kumar, Z. Wei, X. Wu, L. Xu, S. H. Kim, *Mater. Express* **2017**, 7.
- [27] S. Khaleel Basha, K. Vijaya Lakshmi, V. Sugantha Kumari, *Sens. Biosensing Res.* **2016**, 10, 34.
- [28] C. Boissiere, D. Grosso, S. Lepoutre, L. Nicole, A. Brunet Bruneau, C. Sanchez, *Langmuir* **2005**, 21, 12362.
- [29] S. M. Ali, W. A. Farooq, M. R. Baig, M. A. Shar, M. Atif, S. S. Alghamdi, M. S. Algarawi, Naeem-Ur-Rehman, M. H. Aziz, *Mater. Sci.-Poland* **2015**, 33, 601.
- [30] S. Narasimman, L. Balakrishnan, Z. C. Alex, *IEEE Sens. J.* **2018**, 18, 201.
- [31] T. Kavinkumar, S. Manivannann, *Ceramics Int.* **2016**, 42, 1769.
- [32] S. P. Usha, S. K. Mishra, B. D. Gupta, *Materials* **2015**, 8, 2204.
- [33] B. H. Ong, X. Yuan, S. C. Tjin, J. Zhang, H. M. Ng, *Sens. Actuators B* **2006**, 114, 1028.